Journal of Soft Computing in Civil Engineering 8-3 (2024) 49-70

Contents lists available at SCCE

Journal of Soft Computing in Civil Engineering

Journal homepage: www.jsoftcivil.com

A Metaheuristic-Trained Wavelet Neural Network for Predicting of Soil Liquefaction Based on the Standard Penetration Test Results

Ali Reza Ghanizadeh [1*]; **Ahmad Aziminejad** [2]

1. Associate Professor, Department of Civil Engineering, Sirjan University of Technology, Sirjan, Iran
2. Supervision Expert of Construction Projects, Golgohar Mining and Industrial Company, Sirjan, Iran
Corresponding author: *ghanizadeh@sirjantech.ac.ir*

https://doi.org/10.22115/SCCE.2023.408358.1698

ARTICLE INFO

Article history:
Received: 05 August 2023
Revised: 06 October 2023
Accepted: 20 November 2023

Keywords:
Liquefaction;
Wavelet neural network (WNN);
Teaching-learning based optimization (TLBO);
Standard penetration test.

ABSTRACT

Earthquake-induced soil liquefaction is one of the natural hazards that can cause irreparable damages to buildings and infrastructure in addition to threatening human lives. Therefore, accurate prediction of liquefaction has always been one of the important tasks of geotechnical engineers. In the present study, a hybrid approach is introduced to predict liquefaction using the Standard Penetration Test (SPT) results. The approach involves combining Wavelet Neural Network (WNN) and Teaching-Learning Based Optimization (TLBO) techniques to create a binary classification model. The dataset used for this study contains 288 data points, ensuring reliability. The optimal architecture for the WNN is determined as 2-8-1, indicating that it consists of two neurons in the input layer, eight neurons in the hidden layer with the Shannon wavelet function, and one neuron in the output layer with the Hardlim activation function. The developed WNN model is able to predict liquefaction with an overall accuracy of 96.52% based on two input variables, namely modified cyclic stress ratio ($CSR_{7.5}$) and SPT number ($N_{1,60}$). Comparing the accuracy of the WNN-TLBO model developed in this research with that of other artificial intelligence models developed in this field shows the superior accuracy of the WNN-TLBO model compared to previous models.

How to cite this article: Ghanizadeh AR, Aziminejad A. A metaheuristic-trained wavelet neural network for predicting of soil liquefaction based on the standard penetration test results. J Soft Comput Civ Eng 2024;8(3):49–70. https://doi.org/10.22115/scce.2023.408358.1698

2588-2872/ © 2024 The Authors. Published by Pouyan Press.
This is an open access article under the CC BY license (http://creativecommons.org/licenses/by/4.0/).

1. Introduction

Natural disasters such as earthquakes and floods have posed a serious threat to human life and the environment. One of the most destructive phenomena during an earthquake is soil liquefaction (SL). SL occurs when the pressure of the pore-water between individual grains of soil in different layers extremely increases, and eventually, the effective shear strength is greatly decreased to essentially zero, which ultimately causes the transformation of granular soil materials to liquid [1]. SL is usually happened in saturated sandy soils [2,3]. According to laboratory investigations and field observations, liquefaction occurrence depends on different characteristics of earthquake, type and mechanical characteristics of local soil. The soil liquefaction induced by earthquake can cause geo-environmental disasters which lead to extensive damage and engineering failures such as settlements of building and vital urban arterial roads, and ultimately human casualties [4–6]. Recent examples of these types of damages by various earthquakes are the 1999 Kocaeli, the 1999 Chi-Chi, the 2010 Baja California, and the 2011 Tohoku earthquakes [7,8]. Therefore, it is crucial to assess the potential of SL. However, the assessment of SL is a complex challenge since it involves a complex mechanism and is influenced by numerous factors that are interconnected [9].

In the last three decades, many scholars have proposed different methods to predict the occurrence of SL. Traditional techniques used to assess soil resistance to liquefaction include statistical approaches and laboratory experiments like torsional rotation tests, cyclic simple shear tests, and cyclic triaxial tests [10]. However, these methods are time-consuming, expensive, and unreliable due to sampling methods [11,12]. Field test methods such as the cone penetration test (CPT) [13–16], standard penetration test (SPT) [15–18], and shear wave velocity (VS) test [1,19] based on in-situ observations are the most widely used approaches to predict the liquefaction potential. Due to some inherent uncertainties in many of these methods [5,20], it is hard to derive a proper mathematical equation for regression analysis [20–22]. Furthermore, they depend on some “limit states”, established by engineering judgment and field observations, to classify non-liquefaction cases from liquefaction cases [23].

Recent studies have proven that soft computing techniques can establish the “limit state” between non-liquefaction cases from liquefaction cases [9]. Soft computing methods such as support vector machine (SVM) [1,3,5,23–26], artificial neural networks (ANN) [9,11,27–35], and fuzzy neural inference system [35–37] have been widely used in the last 20 years to predict soil liquefaction. For instance, Goh examined the practicality of utilizing various ANN models, like probabilistic neural network and backpropagation neural network (BP), to evaluate liquefaction tendencies by analyzing historical cases [30,31,38]. Juang et al. proposed an ANN to create an empirical equation based on SPT data [15]. In a study, a backpropagation neural network is trained by to determine the liquefaction cyclic resistance ratio based on laboratory data [39]. Pal used an SVM classification method to estimate the potential of SL from actual CPT and SPT data [23]. A Relevance Vector Machine (RVM) is investigated by Samui to predict the occurrence and non-occurrence of SL using actual CPT data [40]. Ramakrishnan et al. utilized an ANN model to predict the liquefaction susceptibility of unconsolidated sediments based on different inputs such as cyclic stress ratio (CSR), liquefaction sensitivity index (LSI),

and cyclic resistance ratio (CRR) [41]. Mughieda et al. studied various ANN models with different inputs to evaluate the earthquake-induced liquefaction potential using CPT data [42]. Farrokhzad et al. developed a BP to create the liquefaction microzonation map for a specific area [43]. Lee and Chern proposed an SVM method for evaluating SL using field records [44]. An RVM model was proposed by Karthikeyan et al. for the prediction of SL using SPT data of Chi–Chi earthquake [45]. Erzin and Ecemis proposed two different ANN models to predict SL using CPT test data [29]. Kohestani et al. introduced a random forest (RF) method based on the classification trees with ensemble learning for CPT-based soil liquefaction assessment [46]. Xue and Yang developed a hybrid SVM and particle swarm optimization (PSO) for the prediction of SL potential [8]. Zhang et al. developed a constrained BP model to assess the potential of SL using SPT test results from 36 earthquakes around the world over 50 years [47].

Although all the above methods are more accurate than statistical approaches, they still suffer from some limitations and exhibit several shortcomings [20]. For instance, kernel-based approaches like SVM and RVM have some disadvantages such as suitable choice of the kernel function, fine-tuning of hyperparameters, and visualization/interpretation of the model [20]. Conventional ANN models also have several shortcomings such as trapping at local minima, over-fitting, and slow convergence. Wavelet neural networks (WNN) overcame the problems of the other types of neural network. For example, WNN needs smaller training samples compared to multi-layer perceptions (MLP). In most of the past researches regarding the development of liquefaction prediction models using soft computing methods, the source code or detailed model for simulation and practical use of the developed models has not been presented.

This paper presents a hybrid model by optimizing the wavelet neural network (WNN) using the teaching learning-based optimization (TLBO) algorithm to assess the potential of SL using the SPT test data. TLBO is utilized to choose the optimal parameters of WNN to improve the performance accuracy for predicting liquefaction. The performance of the WNN-TLBO model has been compared with previous soft computing models (e.g., ANN, SVM, …) in this field. According to authors' knowledge, this research represents the first utilization of WNN architecture in liquefaction prediction using SPT test data. This method can lead to achieve higher prediction accuracy compared to other machine learning methods. Also, in this paper the MATLAB code for implementation of WNN has been provided to predict SL using the developed method.

This paper is organized as follows. Section 2 provides an explanation of the methodologies consisting of WNN and TLBO, and the hybridization of WNN with TLBO. In Section 3, the dataset is described, and the selection of input parameters is discussed. The findings and outcomes are analyzed and discussed in Section 4, and Section 5 offers the concluding remarks of the paper.

2. Methods

This study developed a hybrid model (WNN-TLBO) for the prediction of soil liquefaction potential. A brief description of both WNN architecture and TLBO algorithm and the details of the proposed hybrid WNN-TLBO are described as follows.

2.1. Wavelet neural networks

ANNs are advanced and efficient approaches based on the computational and physical characteristics of the brain[32]. ANNs as reliable computational models can discover complex nonlinear relationships among inputs and output. One of the key advantages of ANNs over conventional empirical and statistical methods is learning without requiring existing knowledge about the nature of the relationships between the inputs and outputs[29]. Many scholars have successfully applied ANNs to various geotechnical problems such as geo-material properties [48–54], bearing capacity of shallow foundations [55,56], bearing capacity of deep foundations [57], seismic liquefaction of soil [58] and slope stability [59,60].

The wavelet neural network (WNN), proposed in 1992 by Zhang and Benveniste [61], is a combination of a neural network and wavelet transform [62]. The wavelet theory was first introduced by Grossman and Morlet in the 1980s [63]. As a mathematical and analysis method, a wavelet transform is actually an advanced form of Fourier series which can perform better than Fourier series to extract time and frequency information from time-series signals.

The architecture of WNN include one input layer, one or more hidden layers, and one output layer. Each layer is formed by several interconnected processing elements known as neurons which are connected to the others on the previous and/or next layer via weights. The hidden layer of WNN consists of the wavelet neurons which process the data. Fig. 1 illustrates the schematic of a typical wavelet neuron. At first, the vector of neuron inputs $X = [x_1, x_2, \dots, x_n]^T$ is multiplied by the connecting weights $W = [w_{1j}, w_{2j}, \dots, w_{nj}]$ between the jth wavelet neuron and the inputs to show the importance of the inputs. The summation block performs the algebraic addition of all the weighted inputs. The weighted sum of the inputs net_j is defined as follows:

$$net_j = \sum_{i=1}^{n} w_{ij}\, x_j \tag{1}$$

where w_{ij} is the connecting weights between the input $i = (1,2, \dots, n)$ and the wavelet neuron j. The weighted sum of the inputs is then passed through the wavelet activation to produce the output signal of the wavelet neuron.

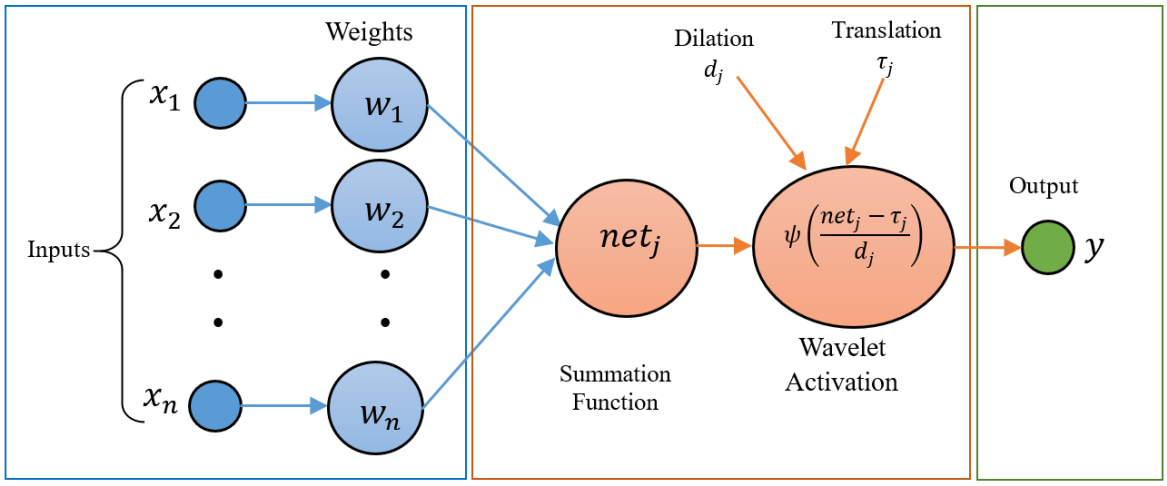

Fig. 1. Schematic of a typical wavelet neuron.

WNN utilizes the wavelet function as the activation function instead of the sigmoid activation function. The wavelet function is made by a series of basic transformations of one function $\psi(x)$, called the "mother wavelet". All daughter wavelets $\psi^{d,\tau}(x)$ are generated by dilation (d) and translation (τ), defined by Eq. (2):

$$\psi^{d,\tau}(x) = \psi\left(\frac{x-\tau}{d}\right) \tag{2}$$

Fig. 2 illustrates the structure of the WNN in this study.

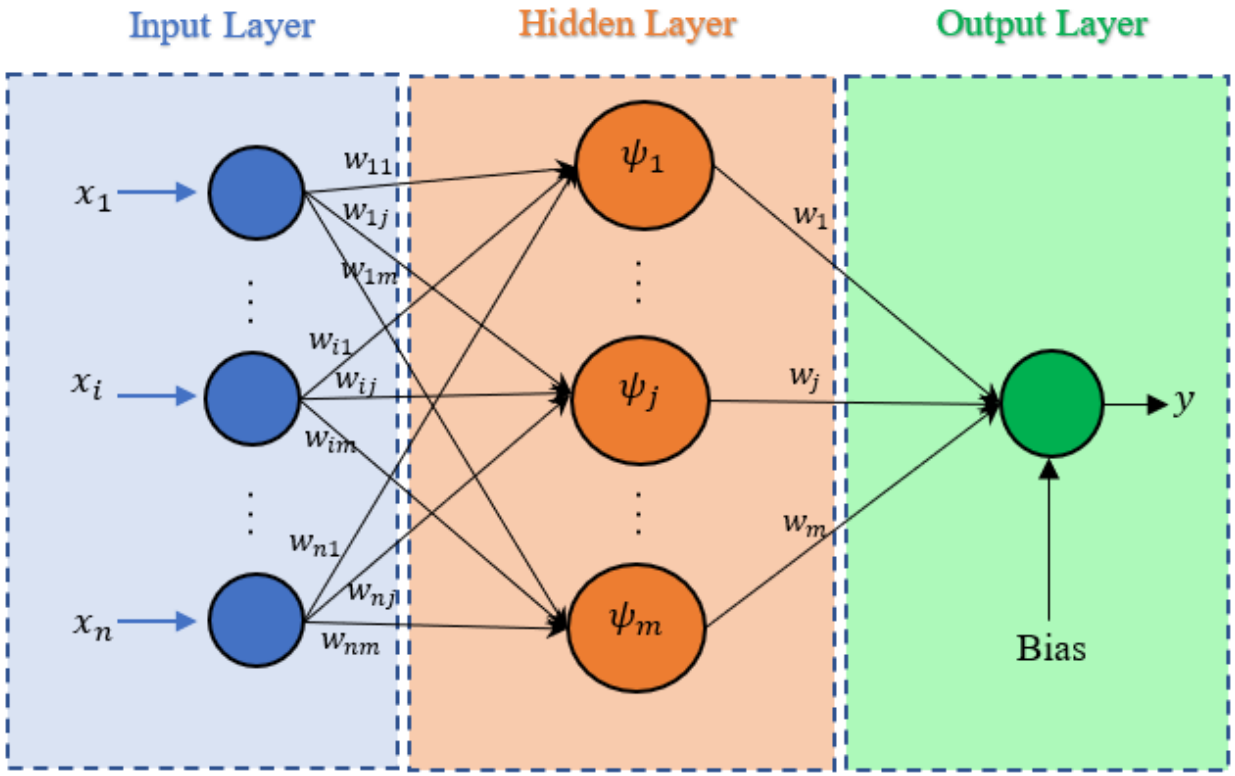

Fig. 2. The architecture of the WNN.

In Fig. 2, the vectors $x_1, x_2, \dots, x_n$ are the vectors of input variables, y is the predicted value (output), w_{ij} is the connecting weight between input neuron i and hidden neuron j, w_j is the connecting weight between hidden neuron j and the output neuron, and ψ_j is the daughter wavelet function of j[th] hidden neuron. The output of the hidden layer $h(j)$ for the input vector $X = [x_1, x_2, \dots, x_n]^T$ is calculated according to Eq. (3) [62]:

$$h(j) = \psi_j^{d_j,\tau_j}\left[\frac{\sum_{i=1}^{n} w_{ij}x_j - \tau_j}{d_j}\right], j = 1,2,\dots,m \tag{3}$$

where $h(j)$ is the output of node j, $\psi_j^{d_j,\tau_j}$ is the daughter wavelet function, w_{ij} is the connecting weight between node i in the input layer and node j in the hidden layer, τ_j is the value of translation, and d_j is the value of the dilation for the wavelet function $\psi_j^{d_j,\tau_j}$. The output y is then computed by Eq. (4):

$$y = Hardlim\left(\sum_{j=1}^{m} w_j h(j) + b\right) \quad (4)$$

where Hardlim is the Hard Limit function as defined in Fig. 3, w_j is the connecting weight between node j in the hidden layer to the output layer, b is the bias term of output neuron, and m is the amount of nodes in the hidden layer [62]. The Hardlim is applied to transfer the output y to either 0 or 1. The occurrence of liquefaction is indicated by 1, while 0 indicates the absence of liquefaction. The Hard Limit transfer function (Fig. 3) is a unit step function used commonly for binary classification. The value changes when the input exceeds a certain threshold.

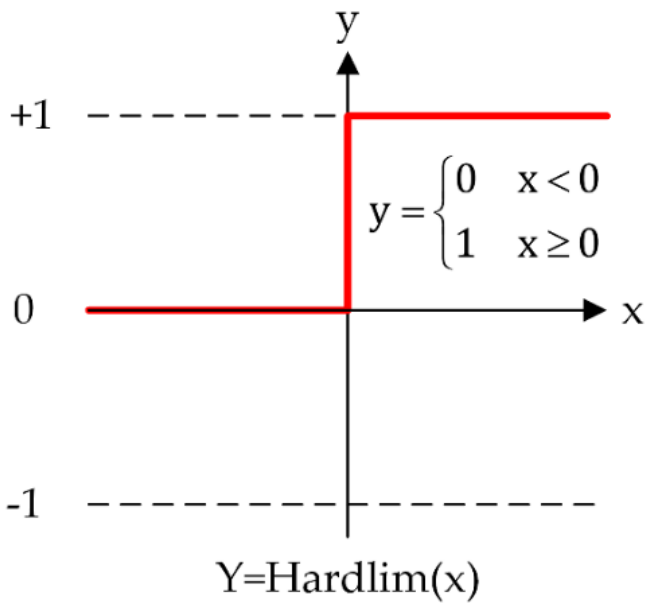

Fig. 3. Hard Limit Function.

The most common wavelet functions are Morlet, Shannon, Mexican Hat, Gaussian, Meyer, GGW, and more [62]. Fig. 4 depicts the formulas and shapes of these wavelet functions.

2.2. Teaching–learning-based optimization (TLBO)

TLBO is a novel metaheuristic optimization algorithm. The concept of TLBO draws inspiration from the dynamics of a classroom, which involves both teachers and students in the learning process [64]. The most important advantages of TLBO over the evolutionary algorithms are simplified numerical structure, high exploration and exploitation, and lack of control parameters, apart from the initial population [65,66]. TLBO involves the random generation of a student population, where the optimization problem considers the different subjects presented to the students as decision variables. The optimization problem considers the students' result as the objective function, with the best result in the entire population being the teacher. TLBO defines two primary modes of learning, including learning by means of the teacher (teaching phase) and learning by means of interaction with the other students (learning phase). Fig. 5 shows the flowchart of TLBO.

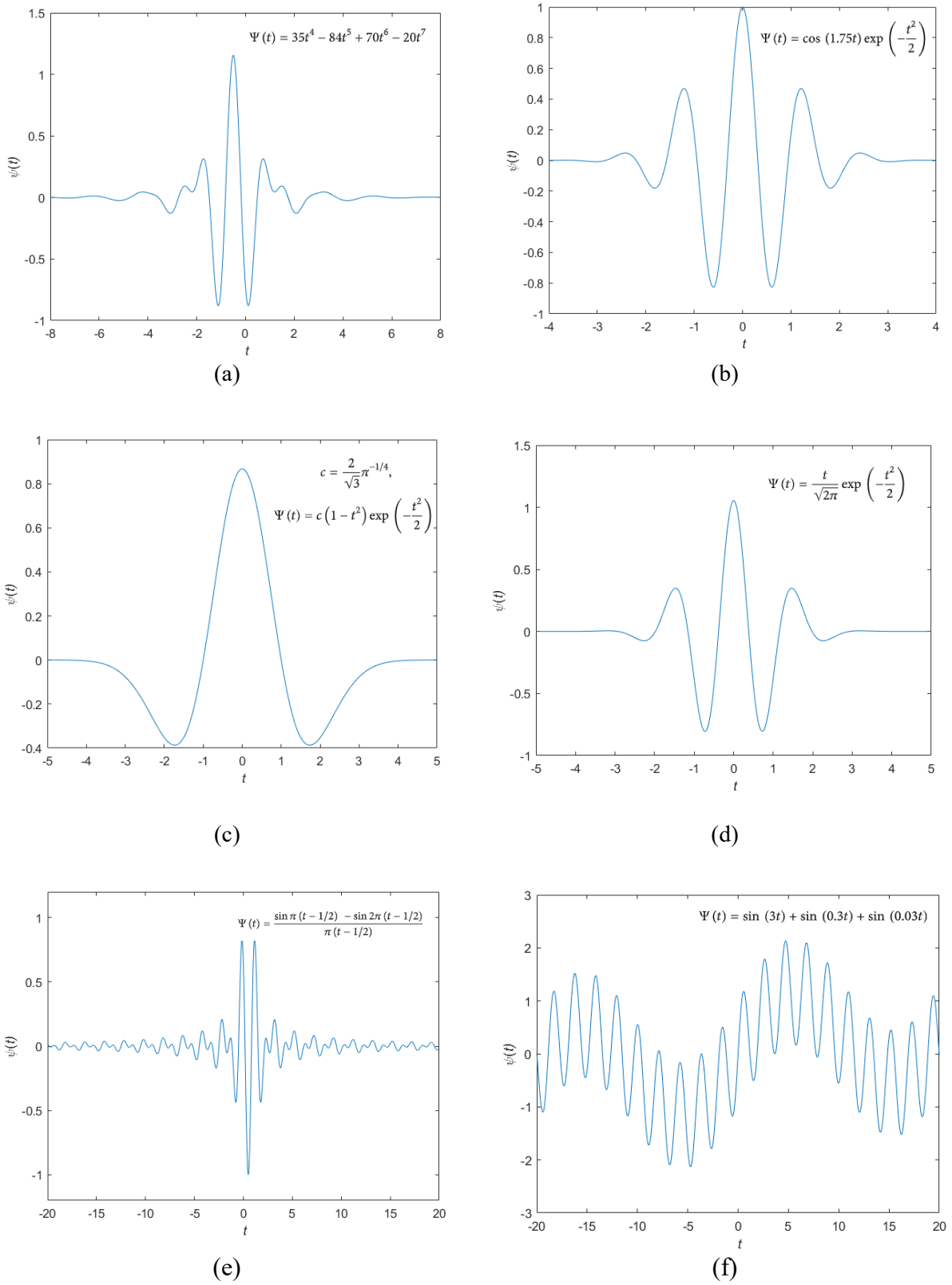

Fig. 4. Wavelet Functions, (a) Meyer, (b) Morlet, (c) Mexican hat, (d) Gaussian, (e) Shannon, (f) GGW.

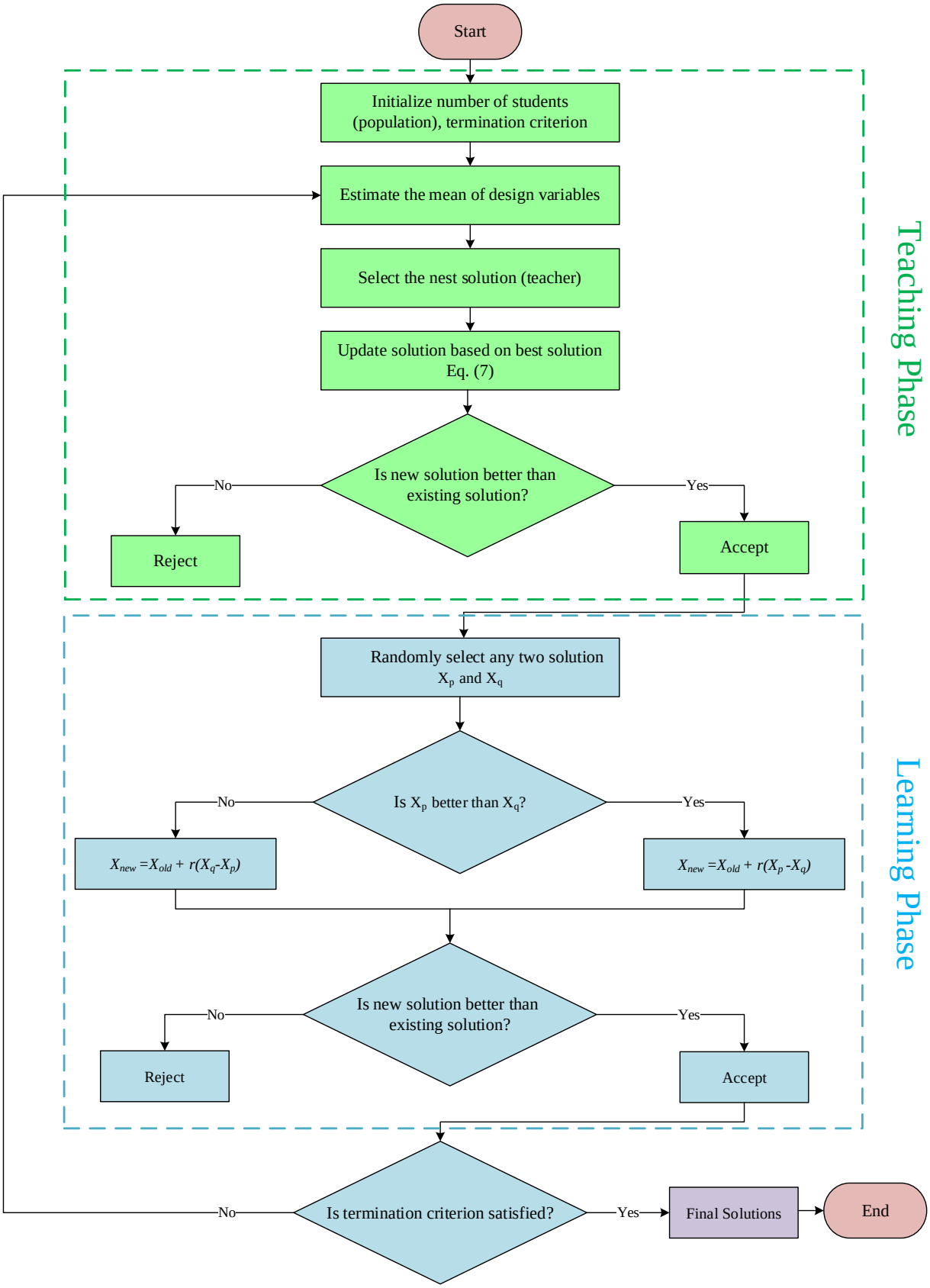

Fig. 5. The flowchart of TLBO.

Teaching Phase: Here, the teacher aims to elevate the knowledges of the students to its level. At first, a teacher is chosen from the population by sorting the values of the fitness function. The teacher in the entire population has the overall influence on the mean result of the entire population of students. At any iteration i, let m be the number of subjects and n be the number of students $(i = 1,2, \dots, n)$, and $M_{j,i}$ be the mean result of the students in a specific subject j. The difference between the result of the teacher T and the mean result of a subject is further calculated by Eq. (5):

$$DM_{j,k,i} = r_i \times \left(X_{j,T,i} - T_F M_{j,i}\right) \tag{5}$$

where $DM_{j,k,i}$ is the difference between the teacher result and the existing mean result for the j^{th} subject in the i^{th} iteration, k is the student index, $X_{j,T,i}$ is the result of the teacher (the best student) for the subject j, r_i is a random number in $[0,1]$, and T_F is the teaching factor calculated as either 1 or 2 by Eq. (6):

$$T_F = round[1 + rand(0,1)\{1,2\}] \tag{6}$$

Based to $DM_{j,k,i}$, the solutions in this phase are updated by Eq. (7):

$$\acute{X}_{j,k,i} = X_{j,k,i} + DM_{j,k,i} \tag{7}$$

where $\acute{X}_{j,k,i}$ is the updated value of $X_{j,k,i}$, and it is accepted only if a better fitness is obtained, i.e., $f\left(\acute{X}_{j,k,i}\right) < f\left(X_{j,k,i}\right)$. All of accepted values are considered as the input for the next phase. The main goal of the teaching phase is to show the students a proper direction to provide global exploration.

Learning Phase: In this phase, a student (learner) randomly tries to interact with other students to enhance its knowledge. Two random students P and Q are selected, so that $X_{j,P,i} \neq X_{j,Q,i}$. The update of the student can be done by Eq. (8):

$$\acute{X}_{j,P,i} = \begin{cases} X_{j,P,i} + r_i\left(X_{j,P,i} - X_{j,Q,i}\right), & if \ \ f\left(X_{j,P,i}\right) < f\left(X_{j,Q,i}\right) \\ X_{j,P,i} + r_i\left(X_{j,Q,i} - X_{j,P,i}\right), & if \ \ f\left(X_{j,Q,i}\right) < f\left(X_{j,P,i}\right) \end{cases} \tag{8}$$

The value of $\acute{X}_{j,P,i}$ is accepted only if it provides a better fitness.

2.3. Hybrid WNN-TLBO

The hybridization of WNN and TLBO is described in this section. The TLBO was utilized to train and optimize the WNN parameters including the connection weights between layers and transformation and dilation of each wavelet neuron in the hidden layer. The performance accuracy of the wavelet neural network is used as the objective function to determine these parameters. The accuracy is calculated by Eq. (9):

$$Performance\ Accuracy\ (\%) = \left(\frac{Number\ of\ Corrected\ Predictions}{Total\ Data}\right) \times 100 \tag{9}$$

Fig. 6 shows the diagram of the proposed WNN-TLBO model to predict the liquefaction potential.

At the beginning, the input data is divided to two training (70%) and testing (30%) sets. Then, for the training procedure, the TLBO parameters are set. In next stage, the weights, dilations, and translations of the WNN are given random values at the start. These values are used to train the WNN, and its accuracy is calculated using by Eq. (9). During the TLBO loop, the goal is to locate and modify the best possible values for the decision variables. This process persists until the maximum number of iterations has been attained.

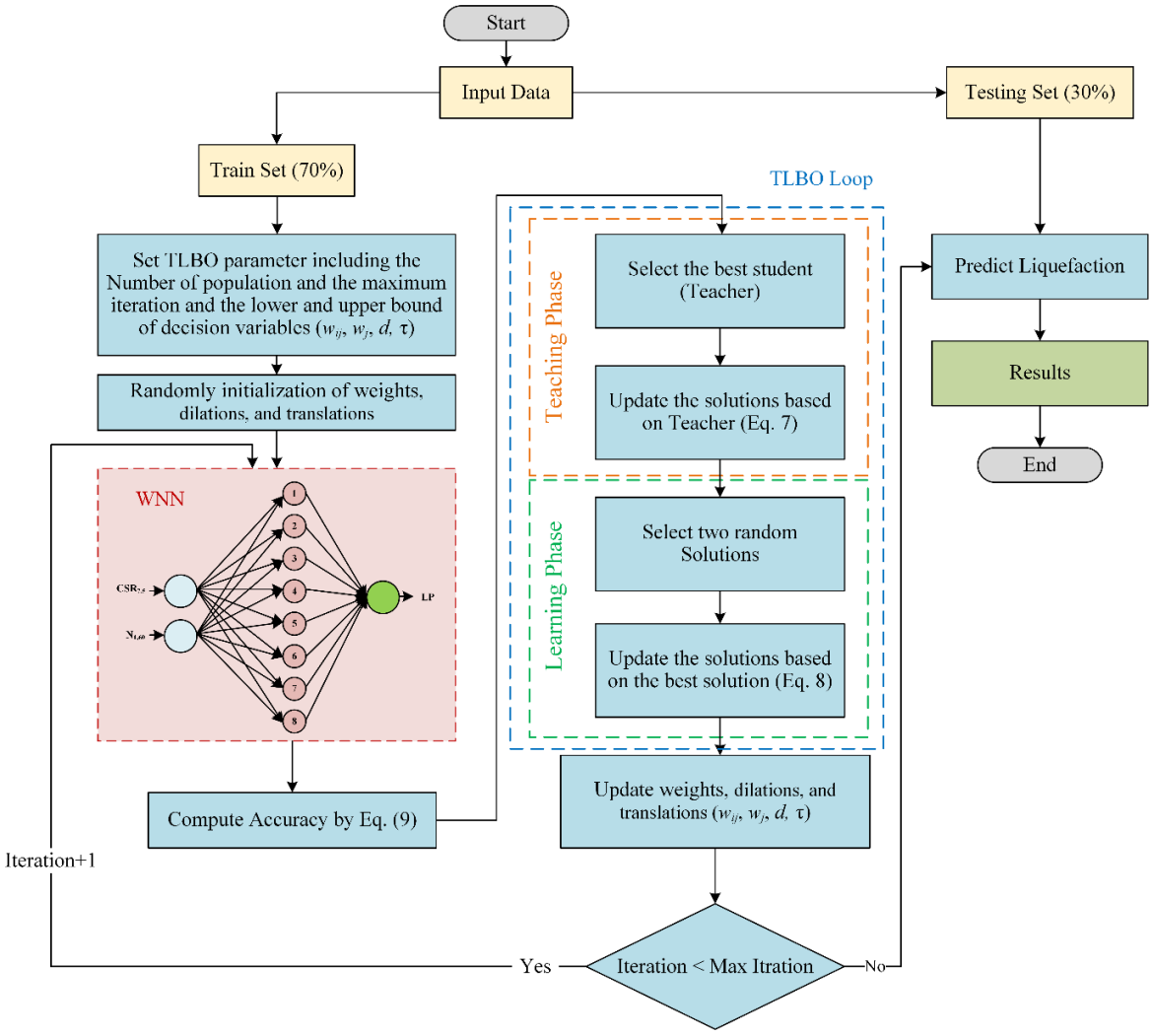
Start
Input Data
Testing Set (30%)
Train Set (70%)
TLBO Loop
Set TLBO parameter including the Number of population and the maximum iteration and the lower and upper bound of decision variables (w_{ij}, w_j, d, τ)
Randomly initialization of weights, dilations, and translations
Teaching Phase
Select the best student (Teacher)
Update the solutions based on Teacher (Eq. 7)
Learning Phase
Select two random Solutions
Update the solutions based on the best solution (Eq. 8)
Predict Liquefaction
Results
End
WNN
LP
Update weights, dilations, and translations (w_{ij}, w_j, d, τ)
Compute Accuracy by Eq. (9)
Iteration+1
Yes
Iteration < Max Itration
No

Fig. 6. The diagram of the WNN-TLBO model.

3. Dataset description

3.1. The SPT dataset

The dataset used in this study includes 288 SPT data from the 1999 Chi-Chi earthquake in Taiwan [67]. Hwang and Yang investigated the Chi-Chi earthquake and the SPT tests results were conducted in the different sites were published [67]. The Richter magnitude of the earthquake ($M_L = 7.3$) is close to the magnitude of 7.5 which is applied in many different liquefaction evaluation methods based on the standard critical periodic resistance curve

approach. More details about the dataset can be found in [67]. Table 1 illustrates the soil and seismic properties of the Chi-Chi earthquake.

The statistical characteristics of the data, such as the minimum, maximum, mean, median, and standard deviation (SD) of each input variable for both the training and testing sets, are presented in Tables 2 and 3. Also, Fig. 7 illustrates the frequency distribution and cumulative frequency percentage of the input parameters, including $N_{1,60}$ and $CSR_{7.5}$. Examination of this information shows that the cumulative frequency percentage of variables is often not uniform and therefore more reliable models can be developed.

Out of 288 data, the liquefied sites are 164 records and the non-liquefied sites are 124 records. Many researchers have used different proportions of records as the training set for various engineering problems [6]. In this study, 70% of the data (202 values) are randomly used as the training set and 30% of data (86 values) are used as the testing set. In the original dataset, the occurrence or non-occurrence of liquefaction is indicated by Yes and No, respectively. These words were changed to values of 1 and 0, respectively, so that they can be used to compare the target with the predicted output during the network training.

Table 1
Soil and seismic and properties of the Chi-Chi earthquake.

Property	Symbol	Range
Critical depth (m)	Critical depth	[1.3,20.3]
Water Table (m)	Water table	[4.0,15.3]
Fine Content (%)	FC	[4,65]
Clay Content (%)	CC	[0,23]
Average grain size (mm)	D_{50}	[0.13,2]
Standard Penetration Value	N_m	[1,50]
Maximum ground acceleration (g)	a_{max}	[0.55,1]
Corrected Standard Penetration Value	$N_{1,60}$	[0.93,49.29]
Cyclic Shear Stress Ratios with a magnitude of 7.5	$CSR_{7.5}$	[0.041,0.82]

Table 2
Statistical descriptions of the training set (202 data) for developing model.

Variables	Max	Min	Mean	Median	SD
$CSR_{7.5}$	0.822	0.041	0. 242	0.172	0.168
$N_{1,60}$	37.49	0.97	12.28	10.64	7.10

Table 3
Statistical descriptions of the testing set (86 data) for developing model.

Variables	Max	Min	Mean	Median	SD
$CSR_{7.5}$	0.790	0.042	0.255	0.186	0.172
$N_{1,60}$	29.49	0.97	91.13	11.54	8.53

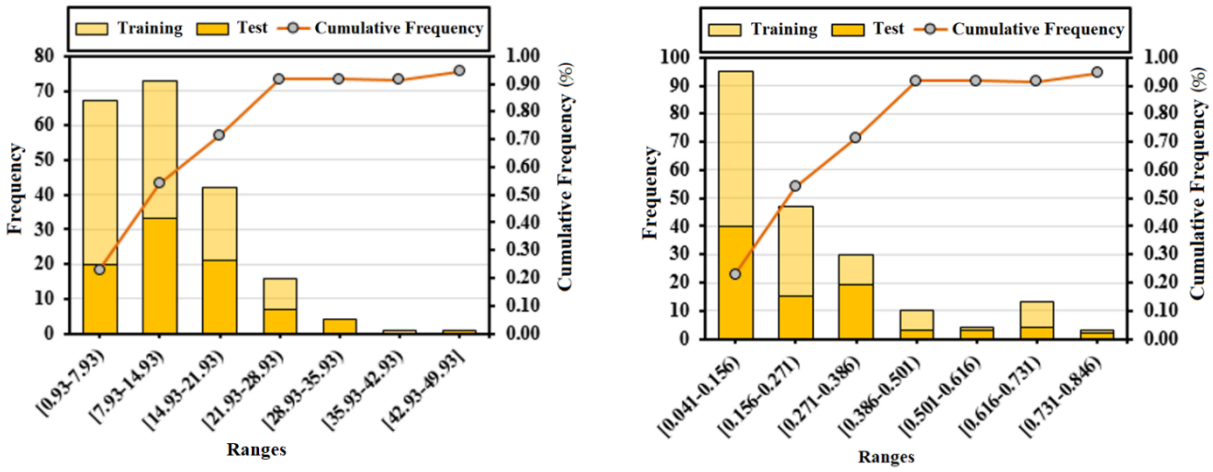

(a) (b)

Fig. 7. Frequency and cumulative frequency histogram of input variables. (a) $N_{1,60}$, (b) $CSR_{7.5}$.

3.2. The choice of parameters

Sensitivity to seismic liquefaction depends on seismic and soil parameters. To be consistent with the previous studies, the corrected SPT value $N_{1,60}$ and the cyclic shear stress ratio $CSR_{7.5}$ are selected as the input variables to the proposed WNN-TLBO model. The $CSR_{7.5}$ variable was selected as an input variable because it is related to other soil and seismic characteristics such as the total vertical stress (σ_v), groundwater table, effective vertical stress at desired depth (σ'_v), stress reduction coefficient (r_d), and the largest horizontal acceleration at ground level (a_{max}).

The general CSR formulation, proposed by [68] and [69], has been adopted with SPT data in the present study with minor modifications. For example, $CSR_{7.5}$ in Eq. (10) corrects earthquakes of different magnitudes to the standard magnitude of 7.5 by utilizing the magnitude scale factor (MSF).

$$CSR_{7.5} = \frac{0.65\left(\frac{\sigma_v}{\sigma'_v}\right)\left(\frac{a_{max}}{g}\right)(r_d)}{MSF} \tag{10}$$

where g is the gravitational acceleration. r_d is previously defined by [69] and is calculated by Eq. (11):

$$r_d = \begin{cases} 1.0 - 0.00765z & for \quad z \leq 9.15m \\ 1.174 - 0.00765z & for \quad 9.15 \leq z \leq 23m \end{cases} \tag{11}$$

where z is the depth below ground surface in meters [69].

MSF is calculated by Eq. (12):

$$MSF = \left(\frac{M_w}{7.5}\right)^{-2.56} \tag{12}$$

where M_w is the magnitude of earthquake.

4. The WNN-TLBO model for prediction of soil liquefaction

The development of the WNN-TLBO to assess soil liquefaction is described in this section. In this regard, MATLAB software was used to develop the WNN-TLBO model.

4.1. The settings of control parameter

Table 4 depicts the setting of the control variables of the WNN-TLBO model. In this study, maximum allowable iteration is considered as the stop criterion.

Table 4
The control parameters of WNN-TLBO.

Parameters	Symbol	Value
Maximum iteration	MaxIt	5000
Number of initial populations	nPop	100
Upper bound of variables	VarMax	+1.5
Lower bound of variables	VarMin	-1.5

4.2. The architecture of WNN-TLBO

In this research, the WNN-TLBO model with one hidden layer has shown reliable results with satisfactory precision. The trial and error method is used to ascertain the appropriate number of neurons in the hidden layer. In this regard, the network was trained and tested using different architectures that encompassed varying numbers of neurons in the hidden layer, ranging from 2 to 20. The most optimal network was obtained with 8 neurons in the hidden layer. The output layer consists of a single neuron that produces an output of 1 to indicate the liquefaction state, and an output of 0 to represent the non-liquefaction state. Therefore, the structure of the proposed network was considered as 2-8-1.

In this study, six wavelet functions consisting of Mexican Hat, Morlet, Gaussian, Meyer, GGW, and Shannon were used in the hidden layer. To determine the most suitable wavelet function for the model, the WNN-TLBO model's optimal architecture was examined, incorporating these wavelet functions. The models were individually executed 10 times using each wavelet activation function, and the top-performing model for every wavelet function was chosen as a potential suitable model. Table 5 shows the accuracy of the wavelet functions.

Table 5
The accuracy of each wavelet function in the WNN-TLBO.

Wavelet Function	Accuracy (%)		
	Training set	Testing set	Overall
Shannon	**96.53**	**96.51**	**96.52**
GGW	95.05	96.51	95.49
Gaussian	96.04	95.34	95.83
Mexican Hat	93.56	95.35	94.10
Meyer	94.55	94.18	94.44
Morlet	94.05	96.51	94.79

The findings indicate that, out of all the wavelet functions, the Shannon wavelet function displays the greatest precision. It attains a precision of 96.53% for the training set, 96.51% for the testing set, and 96.52% for the complete dataset. Therefore, the optimal model selected the Shannon wavelet function as the wavelet function. MATLAB code for simulating the WNN model and optimal values of weights, dilations, translations, and biases can be found in the Appendix.

5. Performance of the WNN-TLBO model

This section focuses on evaluating the performance of the proposed method and comparing the effectiveness of the model against other soft computing methods in assessing SL. The most optimal WNN-TLBO model was achieved using a 2-8-1 architecture and employing the Shannon wavelet function.

Several performance metrics for classification problems such as Precision, Accuracy, Specificity, and Sensitivity were utilized to assess the performance of the proposed model. These performance metrics are extensively utilized for evaluating binary classification tasks [70]. Fig. 8 depicts the confusion matrix along with the equations of the performance metrics. The confusion matrix is a popular evaluation tool in binary classification. It assesses performance by categorizing predictions and actual values into four combinations: false positive (FP), true positive (TP), false negative (FN), and true negative (TN). Here, TP indicates successful and accurate prediction of liquefaction occurrence. FP indicates incorrect prediction of non-liquefaction as liquefaction. TN signifies accurate prediction of non-liquefaction. FN represents incorrect prediction of liquefaction as non-liquefaction.

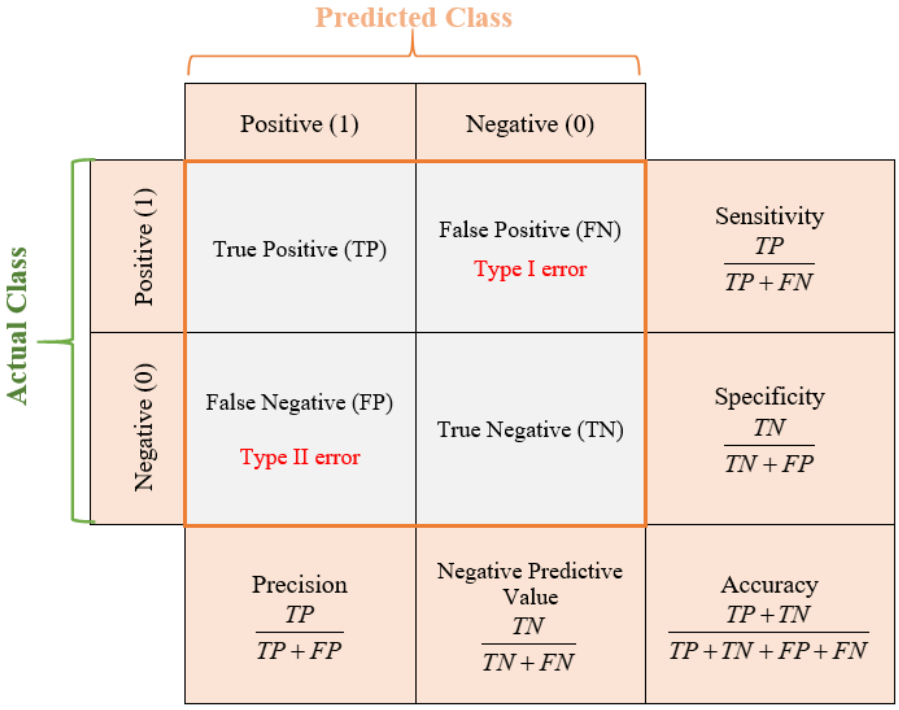

Fig. 8. Confusion Matrix.

Figures 9 and 10 illustrate the performance of the WNN-TLBO model on the training and the testing sets based on the SPT data, respectively. Among 202 cases of the training set, 195 cases were correctly classified (TP=112 and TN=83), and 7 cases were unable to classify (FP=3 and FN=4). Among 86 cases in the testing set, 83 cases were correctly classified (TP=49 and TN=34) and 3 cases were incorrectly classified (FP=1 and FN=2) by the WNN-TLBO model. Table 6 shows the performance metrics of the WNN-TLBO model.

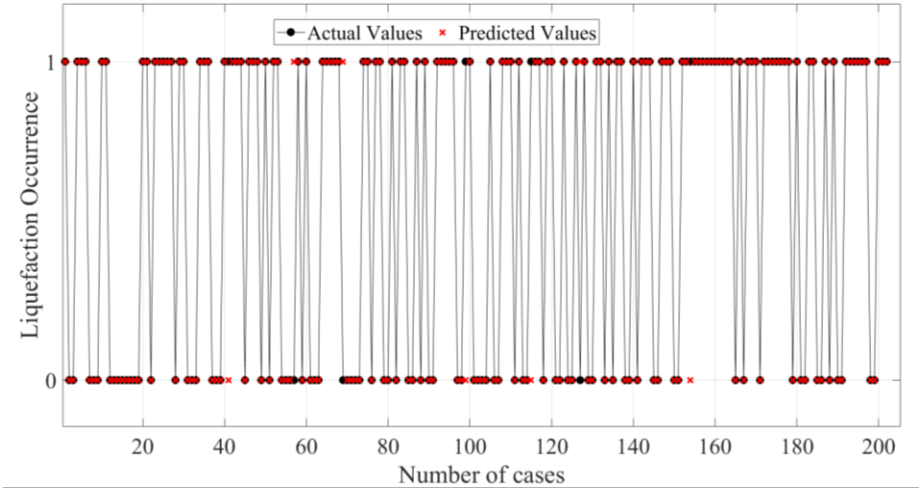

Fig. 9. The classification result of the WNN-TLBO model based on the SPT test data for training set.

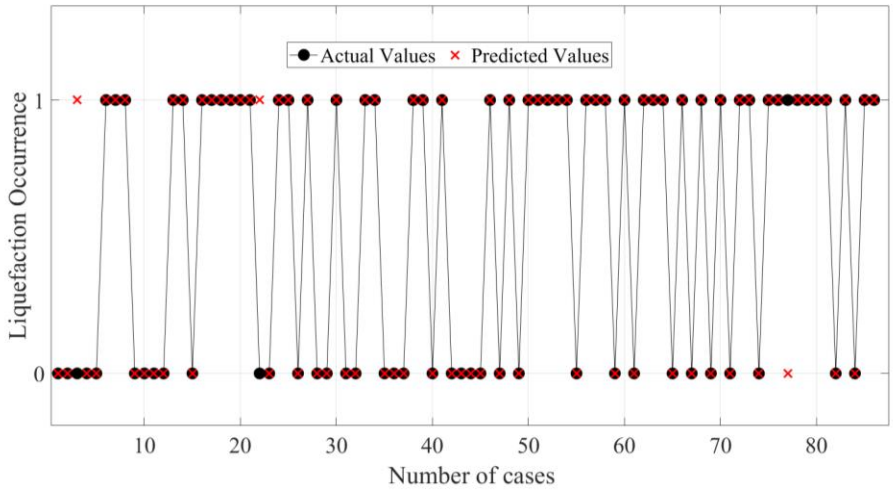

Fig. 10. The classification result of the WNN-TLBO model based on the SPT test data for testing set.

Table 6
The performance metrics of the WNN-TLBO model.

Metrics	Performance Accuracy (%)		
	Training set	Testing set	Overall
Precision	96.55	96.07	96.41
Sensitivity	97.39	98.00	97.57
Specificity	96.71	97.14	96.70
Accuracy	96.53	96.51	96.52

6. Comparison with other soft computing models

In this study, the WNN-TLBO model's performance was assessed by comparing it with other soft computing models in order to determine the effectiveness of the proposed method. For this purpose, three existing models were utilized: the multi-gene genetic programming model (MGGP) [71], ANN [6], RVM [45], and SVM [6]. Similarly, these models adopted a training set comprising 70% of the data (202 values) and a testing set comprising the remaining 30% (86 values).

The ANN based on Multi-layer perceptions (MLP) with the Levenberg Marquardt Backpropagation algorithm was proposed by [6] to assess liquefaction using the SPT dataset. Similar to the present study, two input parameters, including $CSR_{7.5}$ and $N_{1,60}$ were considered in this model. The ANN model has four neurons with a Logsig transfer function in the hidden layer. Moreover, a Tansig transfer function was also utilized in the output layer.

In the SVM model, $CSR_{7.5}$ and $N_{1,60}$ were considered as the input parameters. In addition, a radial basis function was used as the main kernel, in which the values of design parameter C, the width of the radial basis function σ and the number of support vectors were 30, 0.4, and 37, respectively [6].

In the MGGP model, Muduli and Das used a type of genetic programming based on an experimental mathematical model to predict soil liquefaction based on the same SPT dataset [71]. They determined the output parameter based on two input parameters similar to the present study. The optimal result was obtained by 3000 populations with 150 generations with the reproduction probability of 0.05, the crossover probability of 0.85, the mutation probability of 0.1, and the tournament selection of 7. Also, the maximum allowable number of genes and the maximum depth of the GP tree were 3 and 4, respectively.

Moreover, two models based on relevance vector machine (RVM) using the same SPT dataset were used by Karthikeyan et al.[45]. The MODEL I used $CSR_{7.5}$ and $N_{1,60}$ as the input parameters, while MODEL II used peak ground acceleration (PGA) and $N_{1,60}$. The result of the MODEL I was considered as the reference for the comparison in the present study.

Table 7 shows the accuracy of the WNN-TLBO model and the aforementioned model based on the SPT data to assess the liquefaction potential. Since the overall accuracy of each model was not reported in the studies, it was calculated by Eq. (13):

$$Overall\ Accuracy\ (\%) = \frac{Accuracy\ Train \times 70 + Accuracy\ Test \times 30}{100} \tag{13}$$

Table 7
The accuracy comparison of the WNN-TLBO model with the other methods.

Model	Accuracy (%)		
	Train	Test	Overall
SVM	96.04	94.19	95.48
ANN	99.55	88.37	96.19
RVM	96.04	96.51	96.18
MGGP	94.55	94.19	94.44
WNN-TLBO (This study)	**96.53**	**96.51**	**96.52**

As shown in Table 7, the accuracy of the WNN-TLBO for the training set (96.53%) and testing set (96.51%) are better than those of the SVM (96.04%, 94.19%), RVM (96.04%, 96.51%) and MGGP (94.55%, 94.19%) models for the training set and the testing set, respectively. Therefore, the WNN-TLBO had the superior classification performance compared to the SVM and the MGGP models in the training phase, the testing phase, and the overall. Moreover, the accuracy of the WNN-TLBO for the testing set (96.51%) and the overall (96.51%) is better than the accuracy of the ANN model for the testing set (88.37%) and the overall (96.19%). Although the accuracy of the ANN model on the training set is 99.55%, the high difference between the accuracy of the training set (99.55%) and the testing set (88.37%) shows that the model has been over-fitted. Comparison of results obtained by the hybrid WNN-TLBO method with other methods such as ANN, SVM, and MGGP showed that the hybrid WNN-TLBO method can predict the liquefaction potential with a higher accuracy.

7. Conclusions

Evaluating the potential of seismic liquefaction is one of the important aspects of site inspection from the point of view of earthquake risk, so the accuracy of prediction and evaluation of the liquefaction potential is very important. The focus of this research paper is on the development of a hybrid model, combining WNN and TLBO, for predicting liquefaction occurrences. The model takes into account two input variables, namely cyclic stress ratio ($CSR_{7.5}$) and SPT number ($N_{1,60}$). The WNN model was trained and the optimal values for dilation, translation, weights and were determined using the TLBO algorithm in the developed model. A trustworthy dataset consisting of 288 data points was utilized to train the WNN. To identify the most effective WNN structure for seismic liquefaction prediction, various amounts of neurons in the hidden layer and wavelet functions such as Gaussian, Morlet, Mexican Hat, Shannon, Meyer, GGW, and in the hidden layer were explored. The best configuration for the WNN was found to be 2-8-1. This indicates that the optimal WNN consists of two neurons in the input layer, eight neurons in the hidden layer using Shannon wavelet function, and one neuron in the output layer with the Hardlim transfer function. The performance of the WNN-TLBO model was assessed by Accuracy, Precision, Sensitivity, and Specificity. For the training set, the values for these indicators were 96.53%, 96.55%, 97.39%, and 96.71%, respectively. In the testing set, the corresponding values were 96.51%, 96.07%, 98.00%, and 97.14%. When considering the entire dataset, the values were 96.52%, 96.41%, 97.57%, and 96.70%. When comparing the results of the suggested WNN-TLBO model to other methods like SVM, RVM, ANN, and MGGP, it was found that the proposed model outperforms them in terms of accurately predicting the potential for soil liquefaction. WNN, like other artificial intelligence methods, have a restricted scope of effectiveness and primarily depend on the specific case. As a result, its ability to generalize is restrained and they can only be used within the confines of the training data. Nevertheless, the random forest models can be constantly improved by incorporating new data when it becomes accessible. It is suggested that in future research, a more comprehensive and up-to-date database should be used to develop machine learning models for predicting liquefaction based on SPT test results. As another suggestion for further research, it is recommended to use the K-fold cross validation method to validate liquefaction prediction models.

Funding

No funding was received for conducting this study.

Conflicts of Interest

The authors confirm no conflict of interest and there has been no financial support for this study.

Authors contribution statement

A.R.G: Conceptualization; A.A: Data curation; A.R.G, A.A: Formal analysis; A.R.G, A.A: Investigation; A.R.G, A.A: Methodology; A.R.G: Project administration; A.R.G, A.A: Resources; A.R.G, A.A: Software; A.R.G: Supervision; A.R.G: Validation; A.R.G, A.A: Visualization; A.R.G, A.A: Writing – original draft; A.R.G: Writing – review & editing.

Appendix

```
%================================================================================
% Function for predicting of liquefaction Potential based on WNN and SPT results
%================================================================================
% Input includes the input matrix which is a m*n matrix
% m: number of datapoint
% n: number of inputs for each data point
% Input(i,1)= CSR7.5 for datapoint i
% Input(i,2)= N1,60 for datapoint i
% LP=1 indicates the ooccurrence of liquefactin
% LP=0 indicates the absence of liquefaction
function [LP]=LiguiPoten(Inputs)
[m,~]=size(Inputs);

% Input Wights of Hidden Neurons (WNN)
W=[0.364470548217165,-0.381715354277331;1.20973342131062,-0.587324099944053;
    -0.503086016247711,0.188290067210586;-0.912273967771932,-1.25180423641048;
    -1.07988740449946,0.0246884663790783;0.437432061866910,-1.30066373748085;
    -0.822984587797600,0.0553918446612891;0.284893160189390,-0.943257641179222];

% Translation Values of Hidden Neurons (WNN)
t=[1.01525212284545,-0.453371712878006,-0.660507229097132,0.212212518604399,
    0.343817996623739,0.786508160773201,-0.802159460200578,-0.941715358088898];

% 1/Dilation Values of Hidden Neurons (WNN)
d=[0.720177474498582,0.0746543761765446,-0.548008527287282,-1.03444882569153,
    -0.650021677806615,-0.567397739451573,0.706851058888975,-1.00864725421343];

% Weights of Output Neuron (WNN)
Wo=[0.709907161061362,-0.245079790487836,0.0578838922487543,-0.351939230521635,
    -1.40469084755756,-1.06946164070255,0.263323775848642,0.412386914550043];

% Bias Value of Output Neuron (WNN)
bo=[0.0695065901460716];
```

```
%% Start of WNN Simulation
x=W*I';
% Applying Translation
x =bsxfun(@minus, x, t'*ones(1,m));
% Applying Dilations
x =bsxfun(@times, x, d'*ones(1,m));

% Shannon Wavelet Function
H=(sin(pi*(x-0.5))-sin(2*pi*(x-0.5)))./(pi*(x-0.5));
% output of WNN
ww=ones(1,m);
O = Wo*H+bo*ww;
% Hard limit tranfer function
LP=hardlim(O');
%% End of WNN Simulation
End
```

References

[1] Zhou J, Huang S, Wang M, Qiu Y. Performance evaluation of hybrid GA–SVM and GWO–SVM models to predict earthquake-induced liquefaction potential of soil: a multi-dataset investigation. Eng Comput 2022;38:4197–215. https://doi.org/10.1007/s00366-021-01418-3.

[2] Seed HB, Idriss IM. Analysis of Soil Liquefaction: Niigata Earthquake. J Soil Mech Found Div 1967;93:83–108. https://doi.org/10.1061/jsfeaq.0000981.

[3] Xue X, Xiao M. Application of genetic algorithm-based support vector machines for prediction of soil liquefaction. Environ Earth Sci 2016;75:874. https://doi.org/10.1007/s12665-016-5673-7.

[4] Hazout L, El-Abidine Zitouni Z, Belkhatir M, Schanz T. Evaluation of static liquefaction characteristics of saturated loose sand through the mean grain size and extreme grain sizes. Geotech Geol Eng 2017;35:2079–105.

[5] Samui P. Liquefaction prediction using support vector machine model based on cone penetration data. Front Archit Civ Eng China 2013;7:72–82. https://doi.org/10.1007/s11709-013-0185-y.

[6] Samui P, Sitharam TG. Machine learning modelling for predicting soil liquefaction susceptibility. Nat Hazards Earth Syst Sci 2011;11:1–9. https://doi.org/10.5194/nhess-11-1-2011.

[7] Baziar MH, Jafarian Y. Assessment of liquefaction triggering using strain energy concept and ANN model: capacity energy. Soil Dyn Earthq Eng 2007;27:1056–72.

[8] Xue X, Yang X. Seismic liquefaction potential assessed by support vector machines approaches. Bull Eng Geol Environ 2016;75:153–62. https://doi.org/10.1007/s10064-015-0741-x.

[9] Zhang J, Wang Y. An ensemble method to improve prediction of earthquake-induced soil liquefaction: a multi-dataset study. Neural Comput Appl 2021;33:1533–46.

[10] Kurnaz TF, Kaya Y. A novel ensemble model based on GMDH-type neural network for the prediction of CPT-based soil liquefaction. Environ Earth Sci 2019. https://doi.org/10.1007/s12665-019-8344-7.

[11] Alizadeh Mansouri M, Dabiri R. Predicting the liquefaction potential of soil layers in Tabriz city via artificial neural network analysis. vol. 3. Springer International Publishing; 2021. https://doi.org/10.1007/s42452-021-04704-3.

[12] Abo-hashema M. Artificial Neural Network Approach for Overlay Design of Flexible Pavements 2009;6:204–12.

[13] Boulanger RW, Idriss IM. Probabilistic standard penetration test–based liquefaction–triggering procedure. J Geotech Geoenvironmental Eng 2012;138:1185–95.

[14] Guettaya I, El Ouni MR. In situ-based assessment of soil liquefaction potential-case study of an earth dam in Tunisia. Front Struct Civ Eng 2014;8:456–61.

[15] Juang CH, Chen CJ, Jiang T, Andrus RD. Risk-based liquefaction potential evaluation using standard penetration tests. Can Geotech J 2000;37:1195–208.

[16] Vipin KS, Sitharam TG, Anbazhagan P. Probabilistic evaluation of seismic soil liquefaction potential based on SPT data. Nat Hazards 2010;53:547–60.

[17] Jha SK, Suzuki K. Reliability analysis of soil liquefaction based on standard penetration test. Comput Geotech 2009;36:589–96.

[18] Zhang G, Robertson PK, Brachman RWI. Estimating liquefaction-induced lateral displacements using the standard penetration test or cone penetration test. J Geotech Geoenvironmental Eng 2004;130:861–71.

[19] Kayen R, Moss RES, Thompson EM, Seed RB, Cetin KO, Der Kiureghian A, et al. Shear-wave velocity–based probabilistic and deterministic assessment of seismic soil liquefaction potential. J Geotech Geoenvironmental Eng 2013;139:407.

[20] Xue X, Liu E. Seismic liquefaction potential assessed by neural networks. Environ Earth Sci 2017;76:1–15.

[21] Chern S-G, Lee C-Y. CPT-based simplified liquefaction assessment by using fuzzy-neural network. J Mar Sci Technol 2009;17:326–31.

[22] Chern S-G, Lee C-Y, Wang C-C. CPT-based liquefaction assessment by using fuzzy-neural network. J Mar Sci Technol 2008;16:6.

[23] Pal M. Support vector machines-based modelling of seismic liquefaction potential. Int J Numer Anal Methods Geomech 2006;30:983–96.

[24] Rahbarzare A, Azadi M. Improving prediction of soil liquefaction using hybrid optimization algorithms and a fuzzy support vector machine. Bull Eng Geol Environ 2019;78:4977–87. https://doi.org/10.1007/s10064-018-01445-3.

[25] Samui P. Least square support vector machine and relevance vector machine for evaluating seismic liquefaction potential using SPT. Nat Hazards 2011;59:811–22. https://doi.org/10.1007/s11069-011-9797-5.

[26] Zhang Y, Qiu J, Zhang Y, Xie Y. The adoption of a support vector machine optimized by GWO to the prediction of soil liquefaction. Environ Earth Sci 2021;80. https://doi.org/10.1007/s12665-021-09648-w.

[27] Ghanizadeh AR, Aziminejad A, Asteris PG, Armaghani DJ. Soft Computing to Predict Earthquake-Induced Soil Liquefaction via CPT Results. Infrastructures 2023;8:125. https://doi.org/10.3390/infrastructures8080125.

[28] Abbaszadeh Shahri A. Assessment and prediction of liquefaction potential using different artificial neural network models: a case study. Geotech Geol Eng 2016;34:807–15.

[29] Erzin Y, Ecemis N. The use of neural networks for CPT-based liquefaction screening. Bull Eng Geol Environ 2015;74:103–16. https://doi.org/10.1007/s10064-014-0606-8.

[30] Goh ATC. Neural-network modeling of CPT seismic liquefaction data. J Geotech Eng 1996;122:70–3.

[31] Goh ATC. Probabilistic neural network for evaluating seismic liquefaction potential. Can Geotech J 2002;39:219–32.

[32] Hanna AM, Ural D, Saygili G. Neural network model for liquefaction potential in soil deposits using Turkey and Taiwan earthquake data. Soil Dyn Earthq Eng 2007;27:521–40.

[33] Hanna AM, Ural D, Saygili G. Evaluation of liquefaction potential of soil deposits using artificial neural networks. Eng Comput (Swansea, Wales) 2007;24:5–16. https://doi.org/10.1108/02644400710718547.

[34] Kumar D, Samui P, Kim D, Singh A. A Novel Methodology to Classify Soil Liquefaction Using Deep Learning. Geotech Geol Eng 2021;39:1049–58. https://doi.org/10.1007/s10706-020-01544-7.

[35] Venkatesh K, Kumar V, Tiwari RP. Appraisal of liquefaction potential using neural network and neuro fuzzy approach. Appl Artif Intell 2013;27:700–20. https://doi.org/10.1080/08839514.2013.823326.

[36] Kaya Z. Predicting Liquefaction-Induced Lateral Spreading by Using Neural Network and Neuro-Fuzzy Techniques 2016:1–14. https://doi.org/10.1061/(ASCE)GM.1943-5622.0000607.

[37] Xue X, Yang X. Application of the adaptive neuro-fuzzy inference system for prediction of soil liquefaction 2013:901–17. https://doi.org/10.1007/s11069-013-0615-0.

[38] Goh ATC. Seismic liquefaction potential assessed by neural networks. J Geotech Eng 1994;120:1467–80.

[39] Young-Su K, Byung-Tak K. Use of artificial neural networks in the prediction of liquefaction resistance of sands. J Geotech Geoenvironmental Eng 2006;132:1502–4.

[40] Samui P. Seismic liquefaction potential assessment by using relevance vector machine. Earthq Eng Eng Vib 2007;6:331–6.

[41] Ramakrishnan D, Singh TN, Purwar N, Barde KS, Gulati A, Gupta S. Artificial neural network and liquefaction susceptibility assessment: a case study using the 2001 Bhuj earthquake data, Gujarat, India. Comput Geosci 2008;12:491–501.

[42] Mughieda O, Bani-Hani K, Safieh B. Liquefaction assessment by artificial neural networks based on CPT. Int J Geotech Eng 2009;3:289–302.

[43] Little DN. Evaluation of Structural Properties of Lime Stabilized Soils and Aggregates: Mixture Design and Testing Protocol for Lime Stabilized Soils. 2000.

[44] Lee C-Y, Chern S-G. Application of a support vector machine for liquefaction assessment. J Mar Sci Technol 2013;21:10.

[45] Karthikeyan J, Kim D, Aiyer BG, Samui P. SPT-based liquefaction potential assessment by relevance vector machine approach. Eur J Environ Civ Eng 2013;17:248–62.

[46] Kohestani VR, Hassanlourad M, Ardakani A. Evaluation of liquefaction potential based on CPT data using random forest. Nat Hazards 2015;79:1079–89.

[47] Zhang Y, Wang R, Zhang J-M, Zhang J. A constrained neural network model for soil liquefaction assessment with global applicability. Front Struct Civ Eng 2020;14:1066–82.

[48] Bunyamin SA, Ijimdiya TS, Eberemu AO, Osinubi KJ. Artificial Neural Networks Prediction of Compaction Characteristics of Black Cotton Soil Stabilized with Cement Kiln Dust. J Soft Comput Civ Eng 2018;2:50–71. https://doi.org/10.22115/scce.2018.128634.1059.

[49] Ghanizadeh AR, Abbaslou H, Amlashi AT, Alidoust P. Modeling of bentonite/sepiolite plastic concrete compressive strength using artificial neural network and support vector machine. Front Struct Civ Eng 2019;13:215–39. https://doi.org/10.1007/s11709-018-0489-z.

[50] Ghanizadeh AR, Bayat M, Tavana Amlashi, A Rahrovan M. Prediction of Unconfined Compressive Strength of Clay Subgrade Soil Stabilized With Portland Cement and Lime Using Group Method of Data Handling (GMDH). J Transp Infrastruct Eng 2019;5:77–96.

[51] Heidarabadizadeh N, Ghanizadeh AR, Behnood A. Prediction of the resilient modulus of non-cohesive subgrade soils and unbound subbase materials using a hybrid support vector machine method and colliding bodies optimization algorithm. Constr Build Mater 2021;275:122140. https://doi.org/10.1016/j.conbuildmat.2020.122140.

[52] Ghanizadeh AR, Naseralavi SS. Intelligent Prediction of Unconfined Compressive Strength and Young's Modulus of Lean Clay Stabilized with Iron Ore Mine Tailings and Hydrated Lime Using

Gaussian Process Regression. J Soft Comput Civ Eng 2023;7:1–23. https://doi.org/10.22115/scce.2023.370814.1573.

[53] Ghanizadeh AR, Ziaie A, Khatami SMH, Fakharian P. Predicting Resilient Modulus of Clayey Subgrade Soils by Means of Cone Penetration Test Results and Back-Propagation Artificial Neural Network. J Rehabil Civ Eng 2022;10:146–62. https://doi.org/10.22075/JRCE.2022.25013.1568.

[54] Ghanizadeh AR, Delaram A, Fakharian P, Armaghani DJ. Developing Predictive Models of Collapse Settlement and Coefficient of Stress Release of Sandy-Gravel Soil via Evolutionary Polynomial Regression. Appl Sci 2022;12:9986. https://doi.org/10.3390/app12199986.

[55] Khajehzadeh M, Keawsawasvong S, Nehdi ML. Effective Hybrid Soft Computing Approach for Optimum Design of Shallow Foundations. Sustain 2022;14:1–20. https://doi.org/10.3390/su14031847.

[56] Mohammed M, Sharafati A, Al-Ansari N, Yaseen ZM. Shallow foundation settlement quantification: application of hybridized adaptive neuro-fuzzy inference system model. Adv Civ Eng 2020;2020.

[57] Liu W, Tian S, Hu L. Classification of pile foundation integrity based on convolutional neural network. Arab J Geosci 2022;15:793–800.

[58] Bhardwaj RB, Chaurasia SR. Use of ANN, C4. 5 and Random Forest Algorithm in the Evaluation of Seismic Soil Liquefaction. J Soft Comput Civ Eng 2022;6:92–106. https://doi.org/10.22115/SCCE.2022.314762.1380.

[59] Foong LK, Moayedi H. Slope stability evaluation using neural network optimized by equilibrium optimization and vortex search algorithm. Eng Comput 2022;38:1269–83.

[60] Zhang H, Nguyen H, Bui X-N, Pradhan B, Asteris PG, Costache R, et al. A generalized artificial intelligence model for estimating the friction angle of clays in evaluating slope stability using a deep neural network and Harris Hawks optimization algorithm. Eng Comput 2022;38:3901–3914.

[61] Zhang Q, Benveniste A. Wavelet Networks. IEEE Trans Neural Networks 1992;3:889–98. https://doi.org/10.1109/72.165591.

[62] Wang G, Guo L, Duan H. Wavelet Neural Network Using Multiple Wavelet Functions in Target Threat Assessment 2013;2013.

[63] Grossmann A, Morlet J. Decomposition of Hardy functions into square integrable wavelets of constant shape. SIAM J Math Anal 1984;15:723–36.

[64] Rao RV, Savsani VJ, Vakharia DP. Teaching–learning-based optimization: an optimization method for continuous non-linear large scale problems. Inf Sci (Ny) 2012;183:1–15.

[65] Venkata Rao R, Kalyankar VD. Parameter optimization of machining processes using a new optimization algorithm. Mater Manuf Process 2012;27:978–85.

[66] Uzlu E, Kankal M, Akpınar A, Dede T. Estimates of energy consumption in Turkey using neural networks with the teaching–learning-based optimization algorithm. Energy 2014;75:295–303.

[67] Hwang J-H, Yang C-W. Verification of critical cyclic strength curve by Taiwan Chi-Chi earthquake data. Soil Dyn Earthq Eng 2001;21:237–57.

[68] Seed HB, Idriss IM. Simplified procedure for evaluating soil liquefaction potential. J Soil Mech Found Div 1971;97:1249–73.

[69] Youd TL, Idriss IM. Liquefaction resistance of soils: summary report from the 1996 NCEER and 1998 NCEER/NSF workshops on evaluation of liquefaction resistance of soils. J Geotech Geoenvironmental Eng 2001;127:297–313.

[70] De Diego IM, Redondo AR, Fernández RR, Navarro J, Moguerza JM. General Performance Score for classification problems. Appl Intell 2022:1–15.

[71] Muduli PK, Das SK. Evaluation of liquefaction potential of soil based on standard penetration test using multi-gene genetic programming model. Acta Geophys 2014;62:529–43.